



Dynamics of a rolling robot

K. I. Ilin^a, H. K. Moffatt^{b,1}, and V. A. Vladimirov^{a,c}

^aDepartment of Mathematics, University of York, Heslington, York YO10 5DD, United Kingdom; ^bDepartment of Applied Mathematics and Theoretical Physics, University of Cambridge, Cambridge CB3 0WA, United Kingdom; and ^cDepartment of Mathematics and Statistics, Sultan Qaboos University, Muscat 123, Oman

Contributed by H. Keith Moffatt, October 9, 2017 (sent for review August 3, 2017; reviewed by Michal Branicki, Andrzej Herczynski, and Boris Khesin)

Equations describing the rolling of a spherical ball on a horizontal surface are obtained, the motion being activated by an internal rotor driven by a battery mechanism. The rotor is modeled as a point mass mounted inside a spherical shell and caused to move in a prescribed circular orbit relative to the shell. The system is described in terms of four independent dimensionless parameters. The equations governing the angular momentum of the ball relative to the point of contact with the plane constitute a six-dimensional, nonholonomic, nonautonomous dynamical system with cubic nonlinearity. This system is decoupled from a subsidiary system that describes the trajectories of the center of the ball. Numerical integration of these equations for prescribed values of the parameters and initial conditions reveals a tendency toward chaotic behavior as the radius of the circular orbit of the point mass increases (other parameters being held constant). It is further shown that there is a range of values of the initial angular velocity of the shell for which chaotic trajectories are realized while contact between the shell and the plane is maintained. The predicted behavior has been observed in our experiments.

nonholonomic system | internal rotor | chaotic rolling | rolling robot

Introduction

An intriguing toy, known as the “beaver ball,” consists of a rigid hollow sphere, inside which is mounted an eccentric battery-driven rotor. When this ball is placed on the floor with the rotor activated, it rolls in an apparently chaotic manner, a behavior designed to appeal to kittens and mathematicians alike (typical behavior may be seen in [Movies S1–S4](#)). The beaver-ball phenomenon invites the following analysis, which is relevant to a class of problems involving robots with internal mechanisms that can in principle be remotely controlled; indeed the beaver ball may be considered as a simple prototype of such systems. We shall find that, despite the apparent simplicity of the structure of the toy, it admits a wide range of behavior dependent on four governing dimensionless parameters and showing sensitive dependence on initial conditions characteristic of chaotic behavior.

A general procedure for problems of this type involving nonholonomic constraints was described in the seminal paper of Chaplygin (1) [also Neimark and Fufaev (2)]. Application of this procedure for particular problems is, however, exceedingly complex, and we have found it preferable, and physically more revealing for the present problem, to return to first principles, starting simply with linear and angular momentum equations relative to a fixed frame of reference. When these equations are transformed to a suitably defined body frame of reference, a very helpful decoupling of equations determining the angular velocity of the spherical shell and its instantaneous orientation becomes apparent. This decoupling is exploited in the subsequent numerical investigation.

Idealized Model

Consider a rigid uniform spherical shell of mass M and radius a . Suppose that a thin straight rod is mounted within the shell, coinciding with a diameter AB , and on bearings at A and B that allow

free rotation of the rod about its axis (Fig. 1). Let D be a point on AB at distance $d (< a)$ from the center O' of the sphere. Suppose that a second rod DP of length b is rigidly fixed at D perpendicular to AB (with $b^2 + d^2 < a^2$ so that P lies inside the sphere) and that a point mass m is fixed at P . The mass of the rods is assumed negligible compared with either M or m , so the total mass of the ball is just $M + m$. An internal battery mechanism is such that the rod structure APB may be made to rotate about AB with constant angular velocity σ . The ball is placed on a plane horizontal surface, on which it is free to roll without slipping under the influence of gravity g . The problem is then to determine its motion.

We note that this is an oversimplification of the structure of the actual toy beaver ball, since the intrinsic rotational energy of the rotor also contributes to the dynamics. It seems reasonable, however, in the interest of simplicity, to adopt the above idealized model. The relevant dimensionless parameters are

$$\mu = m/M, \quad \gamma = g/\sigma^2 a, \quad \beta = b/a, \quad \delta = d/a, \quad [1]$$

with $\beta^2 + \delta^2 < 1$. Note that $\gamma^{1/2} \equiv n/\sigma$, where $n \equiv (g/a)^{1/2}$ is a natural “gravitational frequency.”

Kinematic Description. Let O be a point fixed in space in the horizontal plane containing the center O' of the sphere. Let $Oxyz$ [with Oz vertically upward, so $\mathbf{g} = (0, 0, -g)$] and $O'x'y'z'$ be Cartesian frames of reference fixed in space and in the body, respectively, and let $O'xyz$ be a moving frame with origin at O' and axes permanently parallel to the axes of $Oxyz$. We may suppose that $O'z'$ is parallel to $O'A$ and that O and O' coincide at time $t = 0$. Let $\mathbf{X} = \overrightarrow{OO'} = (X(t), Y(t), 0)$ with $\mathbf{X}(0) = \mathbf{0}$. The motion of the spherical shell is determined by its angular

Significance

The dynamics of a rolling ball activated by an internal battery mechanism are analyzed by theoretical and numerical techniques. The problem involves four independent dimensionless parameters and is governed by a six-dimensional nonholonomic nonautonomous dynamical system with cubic nonlinearity. It can serve as a prototype for rolling bodies activated by any internal mechanism and is relevant to robotic systems for which such an internal mechanism may be subject to remote control. This is believed to be a unique problem of its kind to have been solved by appeal to fundamental principles of classical dynamics. For this reason, it should be accessible to a wide readership. The numerical results provide clear evidence of both regular and chaotic behavior.

Author contributions: H.K.M. and V.A.V. designed research; K.I.I. and H.K.M. performed research; K.I.I. performed problem formulation and numerical solution; V.A.V. had interactive discussion at all stages of this work; and H.K.M. wrote the paper.

Reviewers: M.B., University of Edinburgh; A.H., Boston College; and B.K., University of Toronto.

The authors declare no conflict of interest.

Published under the [PNAS license](#).

¹To whom correspondence should be addressed. Email: h.k.moffatt@damtp.cam.ac.uk.

This article contains supporting information online at www.pnas.org/lookup/suppl/doi:10.1073/pnas.1713685114/-DCSupplemental.

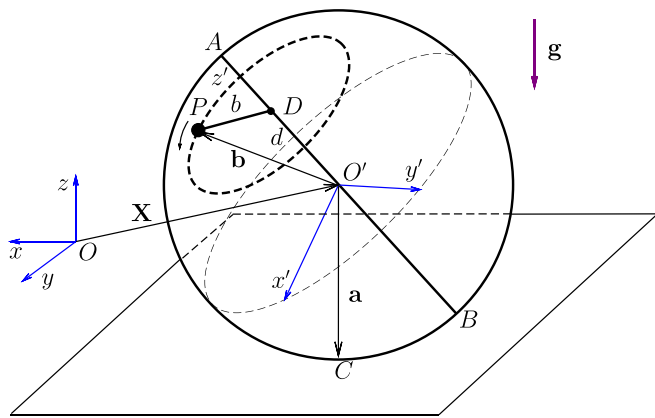


Fig. 1. Configuration sketch. The spherical shell rolls on a horizontal plane; the rod AB is on bearings at A and B that allow it to rotate freely about its axis; the rod DP is rigidly fixed at D at right angles to AB ; a point mass m is fixed at P , and the rod structure APB is driven by a battery mechanism to rotate about AB with constant angular velocity σ ; the axes $O'x'y'z'$ are fixed in the spherical shell.

velocity* $\Omega(t)$ and the velocity $\mathbf{V}(t) = \dot{\mathbf{X}}$ of its center O' . The point of contact C of the sphere with the plane is the vector \mathbf{a} with components $(0, 0, -a)$ in the frame $O'xyz$.

The orientation of the sphere at any time may be described in terms of Euler angles $\{\theta, \phi, \psi\}$, defined [in the “ y convention” of, e.g., Goldstein, Poole, and Safko (3), p. 601] as follows: Starting with $O'x'y'z'$ in coincidence with $O'xyz$ and $O'A$ vertical (i.e., aligned with $O'z'$), rotate $O'x'y'z'$ through an angle ϕ about $O'z'$, then through θ about $O'y'$, and then through ψ about $O'z'$. Then the point \mathbf{x} in $O'xyz$ is the same as the point \mathbf{x}' in $O'x'y'z'$, where

$$\mathbf{x}' = \mathbf{A}\mathbf{x}, \quad [2]$$

and where, with the compact notation $c_\theta \equiv \cos \theta$, $s_\theta \equiv \sin \theta$, etc., the orthogonal transformation matrix \mathbf{A} is given by

$$\mathbf{A} = \begin{bmatrix} -s_\phi s_\psi + c_\theta c_\phi c_\psi & c_\phi s_\psi + c_\theta s_\phi c_\psi & -s_\theta c_\psi \\ -s_\phi c_\psi - c_\theta c_\phi s_\psi & c_\phi c_\psi - c_\theta s_\phi s_\psi & s_\theta s_\psi \\ s_\theta c_\phi & s_\theta s_\phi & c_\theta \end{bmatrix}. \quad [3]$$

The inverse of \mathbf{A} is its transpose \mathbf{A}^T , and $\det \mathbf{A} = +1$.

For any vector \mathbf{h} with components in $O'xyz$, we use the notation $\mathbf{h}' = \mathbf{A}\mathbf{h}$ for the same vector with components in the body frame $O'x'y'z'$. Thus, for example, with

$$\Omega = \left(-\dot{\theta} s_\phi + \dot{\psi} s_\theta c_\phi, \dot{\theta} c_\phi + \dot{\psi} s_\theta s_\phi, \dot{\phi} + \dot{\psi} c_\theta \right), \quad [4]$$

the components of $\Omega' = \mathbf{A}\Omega$ in $O'x'y'z'$ are, as may be verified,

$$\Omega' = \left(\dot{\theta} s_\psi - \dot{\phi} s_\theta c_\psi, \dot{\theta} c_\psi + \dot{\phi} s_\theta s_\psi, \dot{\phi} c_\theta + \dot{\psi} \right). \quad [5]$$

Similarly, with $\mathbf{a} = (0, 0, -a)$,

$$\mathbf{a}' = \mathbf{A}\mathbf{a} = a(\sin \theta \cos \psi, -\sin \theta \sin \psi, -\cos \theta). \quad [6]$$

In the body frame $O'x'y'z'$, the point A has coordinates $(0, 0, a)$, and the mass m moves in the circular orbit

$$\mathbf{b}'(t) = \overrightarrow{O'P} = (b \cos \sigma t, b \sin \sigma t, d) \quad [7]$$

(and then $\mathbf{b} = \mathbf{A}^T \mathbf{b}'$). The important thing here is that $\mathbf{b}'(t)$ is a prescribed function of time. The method that follows can be used for any other prescription of $\mathbf{b}'(t)$ and can be generalized to any

number of masses $\{m_1, m_2, m_3, \dots\}$ with prescribed trajectories in $O'x'y'z'$, $\{\mathbf{b}'_1(t), \mathbf{b}'_2(t), \mathbf{b}'_3(t) \dots\}$.

Now the position vector of the mass m in the frame $Oxyz$ is given by $\mathbf{x}_m = \mathbf{X} + \mathbf{b}$, and its velocity in this frame is

$$\mathbf{v}_m = \dot{\mathbf{X}} + \dot{\mathbf{b}} = \mathbf{V} + \mathbf{v}, \quad \text{say.} \quad [8]$$

Relative to the body frame $O'x'y'z'$, the velocity of m is

$$\mathbf{v}'_m = \mathbf{V}' + \mathbf{v}' = D\mathbf{X}' + D\mathbf{b}', \quad [9]$$

where the operator D is defined for any vector $\mathbf{h}'(t)$ by

$$D\mathbf{h}' \equiv \dot{\mathbf{h}}' + \Omega' \times \mathbf{h}',$$

and the dot represents time differentiation. In particular, $\dot{\Omega}' = \dot{\Omega}'$. Note further that, since $\mathbf{a} = (0, 0, -a)$ is constant,

$$\dot{\mathbf{a}} \equiv \dot{\mathbf{a}}' + \Omega' \times \mathbf{a}' = 0, \quad [10]$$

with the obvious first integral $|\mathbf{a}'|^2 = \text{cst}$. Finally, note that

$$D\mathbf{b}' = \dot{\mathbf{b}}' + \Omega' \times \mathbf{b}', \quad [11]$$

$$D^2\mathbf{b}' = \ddot{\mathbf{b}}' + \Omega' \times (\Omega' \times \mathbf{b}') + 2\Omega' \times \dot{\mathbf{b}}' + \dot{\Omega}' \times \mathbf{b}'. \quad [12]$$

Here, $\Omega' \times (\Omega' \times \mathbf{b}')$ is the centrifugal acceleration and $2\Omega' \times \dot{\mathbf{b}}'$ the Coriolis acceleration. The term $\dot{\Omega}' \times \mathbf{b}'$ is known as the Poincaré acceleration in astronomical contexts.

Rolling and Contact Conditions. The rolling condition (a nonholonomic constraint) expresses the fact that the point C of the spherical shell is instantaneously at rest for all t ; i.e.,

$$\mathbf{V} + \Omega \times \mathbf{a} = 0 \quad \text{and so also} \quad \dot{\mathbf{V}} = \mathbf{a} \times \dot{\Omega}. \quad [13]$$

The forces acting on the ball are its weight $(M + m)\mathbf{g}$ and the force $\mathbf{F} = (F_x, F_y, F_z)$ at the point of contact C . The frictional contribution $(F_x, F_y, 0)$ serves simply to maintain the rolling conditions [13]. The normal contribution $(0, 0, F_z)$ prevents vertical motion of the center O' , and we must require that $F_z > 0$ for all t to ensure permanent contact with the plane. Since the maximum upward force on the ball due to the rotation of the mass m is of order $mb\sigma^2$, we may expect that contact will be maintained

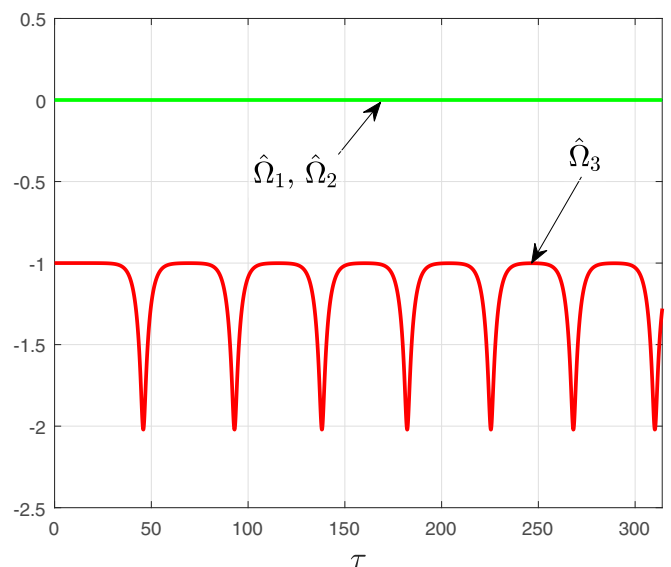


Fig. 2. Components of $\hat{\Omega}$ vs. τ from numerical solution of Eq. 36, with $\mu = 1$, $\gamma = 1$, $\delta = 0$, and $\beta = 1/2$ and with initial conditions $\hat{\Omega}(0) = (0, 0, -1)$, $\hat{\mathbf{a}}(0) = (-1, 0, 0)$.

*The list (1) of dimensionless parameters may be supplemented by the parameter Ω_0/σ , where $\Omega_0 = |\Omega(0)|$ is determined by initial conditions.

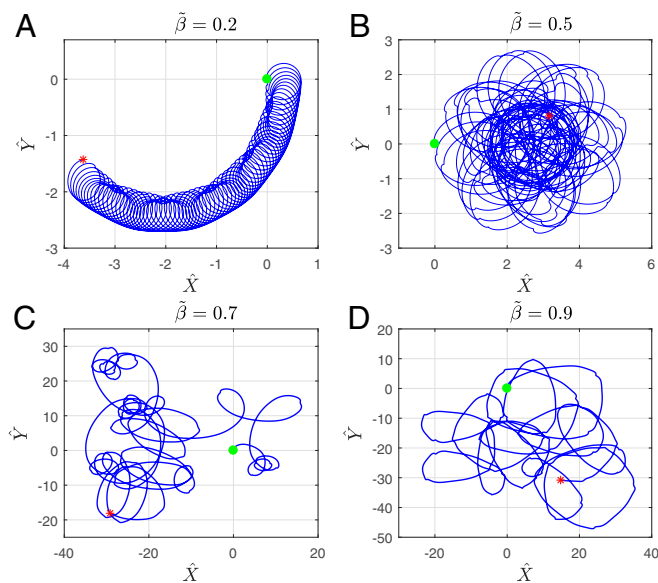


Fig. 3. Trajectories $\mathbf{X}(\tau)$ of the ball center for $\mu = 1$, $\gamma = 1$, $\rho = 1/2$, $\tilde{\beta}$ as shown, and δ given by Eq. 40, with initial conditions 41 and 42. (A–D) Lyapunov exponents (A) $\lambda \approx 0.002$, (B) $\lambda \approx 0.003$, (C) $\lambda \approx 0.053$, and (D) $\lambda \approx 0.077$.

provided $(M + m)g \gtrsim mb\sigma^2$ or, in terms of the dimensionless parameters (1), provided

$$(1 + \mu)\gamma \gtrsim \mu\beta. \quad [14]$$

This condition is refined in Eq. 35 below.

Equations of Motion. We consider now the equations for the rate of change of the linear momentum of the system,

$$\dot{\mathbf{p}} = M\mathbf{V} + m\mathbf{v}_m, \quad [15]$$

and of its angular momentum relative to the point O ,

$$\begin{aligned} \dot{\mathbf{L}} &= \mathbf{X} \times M\mathbf{V} + (\mathbf{X} + \mathbf{b}) \times m\mathbf{v}_m + I\dot{\boldsymbol{\Omega}} \\ &= \mathbf{X} \times \dot{\mathbf{p}} + m\mathbf{b} \times \mathbf{v}_m + I\dot{\boldsymbol{\Omega}}, \end{aligned} \quad [16]$$

where I is the moment of inertia of the shell. These equations are

$$\dot{\mathbf{p}} = (M + m)\mathbf{g} + \mathbf{F}, \quad [17]$$

and

$$\dot{\mathbf{L}} = \mathbf{X} \times M\mathbf{g} + (\mathbf{X} + \mathbf{b}) \times m\mathbf{g} + (\mathbf{X} + \mathbf{a}) \times \mathbf{F}. \quad [18]$$

Using Eq. 16 and Eqs. 17 and 18 can be written in the form

$$I\dot{\boldsymbol{\Omega}} + m\mathbf{b} \times \dot{\mathbf{v}}_m = m\mathbf{b} \times \mathbf{g} + \mathbf{a} \times \mathbf{F}. \quad [19]$$

Eliminating \mathbf{F} from Eqs. 17 and 19, and using Eq. 15, we obtain

$$I\dot{\boldsymbol{\Omega}} - M\mathbf{a} \times \dot{\mathbf{V}} + m\mathbf{s} \times \dot{\mathbf{v}}_m = m\mathbf{b} \times \mathbf{g}, \quad [20]$$

where $\mathbf{s} = \mathbf{b} - \mathbf{a}$. Now we eliminate \mathbf{V} from Eq. 20 using the rolling conditions 13 and $\mathbf{v}_m = \mathbf{V} + \mathbf{v}$. After simplification, this gives

$$I\dot{\boldsymbol{\Omega}} - M\mathbf{a} \times (\mathbf{a} \times \dot{\boldsymbol{\Omega}}) + m\mathbf{s} \times (\mathbf{a} \times \dot{\boldsymbol{\Omega}}) + m\mathbf{s} \times \dot{\mathbf{v}} = m\mathbf{b} \times \mathbf{g}. \quad [21]$$

This equation describes the rate of change of angular momentum of the ball relative to the point C of the shell, which is instantaneously at rest.

So far, we have expressed these dynamical equations in the rest frame $Oxyz$. However, since the motion of the point P in the body frame $O'x'y'z'$ is known, it makes sense to rewrite [21] relative to the body frame. As this is a vector equation, it holds equally in the body frame, with \mathbf{a} replaced by \mathbf{a}' and similarly for

the other vectors in the equation. Using the fact that $\mathbf{g} = n^2\mathbf{a}$, the plane being horizontal, the transformed equation is

$$\begin{aligned} I\dot{\boldsymbol{\Omega}}' - M\mathbf{a}' \times (\mathbf{a}' \times \dot{\boldsymbol{\Omega}}') + m\mathbf{s}' \times (\mathbf{a}' \times \dot{\boldsymbol{\Omega}}') \\ + m\mathbf{s}' \times D^2\mathbf{b}' = mn^2\mathbf{b}' \times \mathbf{a}'. \end{aligned} \quad [22]$$

Noting Eq. 12, and bringing all of the terms involving $\dot{\boldsymbol{\Omega}}'$ to the left, this equation takes the form

$$\begin{aligned} m^{-1}\mathbf{Q}\dot{\boldsymbol{\Omega}}' = -\mathbf{s}' \times \dot{\mathbf{b}}' - 2\mathbf{s}' \times (\boldsymbol{\Omega}' \times \dot{\mathbf{b}}') \\ - (\mathbf{b}' \cdot \boldsymbol{\Omega}') (\mathbf{s}' \times \boldsymbol{\Omega}') + (n^2 + \boldsymbol{\Omega}'^2) \mathbf{b}' \times \mathbf{a}', \end{aligned} \quad [23]$$

where \mathbf{Q} is the symmetric matrix with elements

$$Q_{ik} = (I + Ma^2 + m\mathbf{s}'^2) \delta_{ik} - Ma'_i a'_k - ms'_i s'_k. \quad [24]$$

Note that \mathbf{Q} is positive definite, given that $I > 0$. When coupled with Eq. 10, i.e., with

$$\dot{\mathbf{a}}' + \boldsymbol{\Omega}' \times \mathbf{a}' = 0, \quad [25]$$

Eqs. 23–25 constitute a six-dimensional, nonautonomous, non-holonomic dynamical system, with cubic nonlinearity[†], for the components of $\mathbf{a}'(t)$ and $\boldsymbol{\Omega}'(t)$, having the obvious first integral $\mathbf{a}'^2 = a^2 = \text{cst}$. It is noteworthy that this system is decoupled from Eq. 5, which in principle determines the evolution of the Euler angles $\{\theta(t), \phi(t), \psi(t)\}$, once $\boldsymbol{\Omega}'(t)$ is known. We do not, however, need to determine these Euler angles, which is fortunate because if θ approaches zero, the angles ϕ and ψ become indeterminate.

Nondimensionalization. From this point on, we take $I = \frac{2}{3}Ma^2$, the value for a thin spherical shell, so $I + Ma^2 = \frac{5}{3}Ma^2$. With dimensionless variables defined by[‡]

$$\tau = \sigma t, \quad \hat{\boldsymbol{\Omega}} = \boldsymbol{\Omega}'/\sigma, \quad \hat{\mathbf{a}} = \mathbf{a}'/a, \quad \hat{\mathbf{b}} = \mathbf{b}'/a, \quad \hat{\mathbf{s}} = \mathbf{s}' - \hat{\mathbf{a}}, \quad [26]$$

Eqs. 23–25 take the form

$$\begin{aligned} \mu^{-1}\hat{\mathbf{Q}}\dot{\hat{\boldsymbol{\Omega}}} = -\hat{\mathbf{s}} \times \hat{\mathbf{b}}_{\tau\tau} - 2\hat{\mathbf{s}} \times (\hat{\boldsymbol{\Omega}} \times \hat{\mathbf{b}}_{\tau}) \\ - (\hat{\mathbf{b}} \cdot \hat{\boldsymbol{\Omega}}) (\hat{\mathbf{s}} \times \hat{\boldsymbol{\Omega}}) + (\gamma + \hat{\boldsymbol{\Omega}}^2) \hat{\mathbf{b}} \times \hat{\mathbf{a}}, \end{aligned} \quad [27]$$

$$\dot{\hat{\mathbf{a}}} = \hat{\mathbf{a}} \times \hat{\boldsymbol{\Omega}}, \quad [28]$$

where now $\hat{\mathbf{Q}}$ is the matrix with elements

$$\hat{Q}_{ik} = \left(\frac{5}{3} + \mu\hat{\mathbf{s}}^2\right) \delta_{ik} - \hat{a}_i \hat{a}_k - \mu\hat{s}_i \hat{s}_k, \quad [29]$$

and where, from Eq. 7, the orbit of the mass m is now prescribed as

$$\hat{\mathbf{b}} = (\beta \cos \tau, \beta \sin \tau, \delta). \quad [30]$$

As expected, Eqs. 27–30 contain the four dimensionless parameters μ , γ , β , and δ defined by Eq. 1.

The Trajectory $\mathbf{X}(\tau)$ of the Ball.

To determine the trajectory $\mathbf{X}(\tau)$ of the ball, it is not enough to solve Eqs. 27 and 28: We also need to integrate the rolling condition $\dot{\mathbf{X}} = \mathbf{a} \times \boldsymbol{\Omega}$. We may again bypass the Euler angles as follows. Let \mathbf{e}_1 and \mathbf{e}_2 be unit vectors along the coordinate axes $O'x$ and $O'y$. Then \mathbf{e}'_1 and \mathbf{e}'_2 (the same vectors relative to the rotating axes) satisfy the equations

$$\mathbf{e}'_{1\tau} = \mathbf{e}'_1 \times \hat{\boldsymbol{\Omega}}, \quad \mathbf{e}'_{2\tau} = \mathbf{e}'_2 \times \hat{\boldsymbol{\Omega}}. \quad [31]$$

[†] This cubic nonlinearity is evident, e.g., in the term $\boldsymbol{\Omega}'^2 \mathbf{b}' \times \mathbf{a}'$ of Eq. 23 in which $\mathbf{b}'(t)$ is prescribed.

[‡] Alternatively, we may define $\hat{\boldsymbol{\Omega}} = \boldsymbol{\Omega}'/n = \gamma^{-1/2}\boldsymbol{\Omega}'$, with corresponding adjustments in Eqs. 27 and 28.

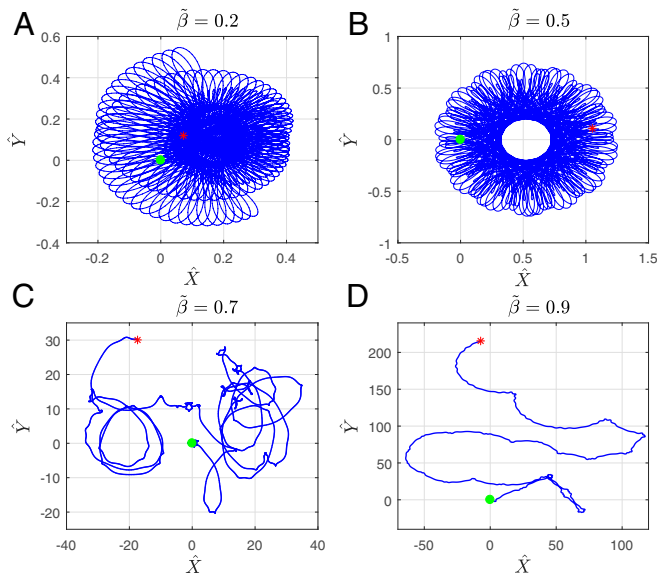


Fig. 4. Same as Fig. 3, but with initial conditions given by Eqs. 41 and 43. (A) $\lambda \approx 0.002$, (B) $\lambda \approx 0.003$, (C) $\lambda \approx 0.102$, and (D) $\lambda \approx 0.059$.

Having solved these, $X(\tau)$ and $Y(\tau)$ (nondimensionalized with a) are determined by integration of the components of Eq. 13; noting that the scalar product of any two vectors is frame-independent, these give

$$X_\tau = \sigma^{-1} \Omega \cdot \mathbf{e}_2 = \hat{\Omega} \cdot \mathbf{e}'_2, \quad Y_\tau = -\sigma^{-1} \Omega \cdot \mathbf{e}_1 = -\hat{\Omega} \cdot \mathbf{e}'_1, \quad [32]$$

and, with the right-hand sides now known, direct numerical integration is straightforward.

The Precise Contact Condition. With $\mathbf{V} \cdot \mathbf{e}_3 = 0$, and $\mathbf{v}_m \cdot \mathbf{e}_3 = \mathbf{v} \cdot \mathbf{e}_3$, where $\mathbf{e}_3 = (0, 0, 1)$, the vertical component of Eq. 17 gives

$$\begin{aligned} F_z &= (M + m)g + m \frac{d}{dt}(\mathbf{v} \cdot \mathbf{e}_3) \\ &= (M + m)g + m \frac{d}{dt}(\mathbf{v}' \cdot \mathbf{e}'_3), \end{aligned} \quad [33]$$

using again the invariance of the scalar product. Now, with $\mathbf{v}' = D\mathbf{b}'$ and $\mathbf{e}'_3 = \mathbf{e}_3 \times \Omega'$, we have

$$\frac{d}{dt}(\mathbf{v}' \cdot \mathbf{e}'_3) = \mathbf{e}'_3 \cdot \left[\frac{d}{dt}(D\mathbf{b}') + \Omega' \times D\mathbf{b}' \right] = \mathbf{e}'_3 \cdot D^2\mathbf{b}', \quad [34]$$

where $D^2\mathbf{b}'$ is given by Eq. 12. Contact between the sphere and the plane is maintained provided $F_z > 0$. Hence, in dimensionless terms, with $\mathbf{e}'_3 = -\hat{\mathbf{a}}$, this contact condition becomes

$$(1 + \mu)\gamma > \mu\hat{\mathbf{a}} \cdot D^2\mathbf{b}', \quad [35]$$

a condition that is satisfied provided γ is large enough; just how large it must be can be determined when $\hat{\mathbf{a}}(t)$ and $\hat{\Omega}(t)$ are known, i.e., after Eqs. 27 and 28 have been solved. The criterion 35 provides the required refinement of Eq. 14.

Particular Cases

i) Axisymmetric Ball. If $\beta = 0$ in Eq. 30, the mass m is fixed on the diameter AB , and the ball is axisymmetric about this diameter. This is a well-known integrable case [Chaplygin (1)].

ii) One-Dimensional Time-Periodic Solutions When $\delta = 0$. In this case D coincides with O' and the rod DP rotates in a diametral plane, and it is clear that there must exist time-periodic solutions for which the rod AB remains horizontal and the ball

rolls in the y direction perpendicular to AB . For this type of solution,

$$\hat{\Omega}(\tau) = (0, 0, \hat{\Omega}_3(\tau)) \quad \text{and} \quad \hat{\mathbf{a}}(\tau) = (\hat{a}_1(\tau), \hat{a}_2(\tau), 0),$$

and Eqs. 27 and 28 simplify to

$$\begin{aligned} \left(\frac{5}{3} + \mu\hat{s}^2 \right) \hat{\Omega}_{3\tau} &= -\mu\beta(\hat{a}_1 \sin \tau - \hat{a}_2 \cos \tau) \left(\gamma + (1 + \hat{\Omega}_3)^2 \right), \\ \hat{a}_{1\tau} &= \hat{\Omega}_3 \hat{a}_2, \quad \hat{a}_{2\tau} = -\hat{\Omega}_3 \hat{a}_1, \end{aligned} \quad [36]$$

a 3D dynamical system with periodic coefficients. In general this cannot be solved analytically; there are, however, two exact solutions given by

$$\hat{\Omega}_3(\tau) = -1, \quad \hat{a}_1 = \pm \cos \tau, \quad \hat{a}_2 = \pm \sin \tau, \quad [37]$$

which correspond to steady rolling of the ball, with P either vertically below or above O' (\pm signs in Eq. 37, respectively). The former solution is presumably stable and the latter unstable. For these solutions, the mass m is at rest relative to the center of the shell, its rotation relative to the shell being exactly compensated by reverse rolling of the shell with the same frequency σ .

More generally, numerical solution of Eq. 36 using MATLAB shows that although the trajectory of the ball is a straight line, its velocity oscillates with time as the mass m rises and falls. Fig. 2 shows the function $\hat{\Omega}_3(\tau)$, which, starting very near the unstable solution, quickly becomes a periodic function of τ , although (like an unstable compound pendulum) remaining for some time during each cycle in a close neighborhood of the unstable configuration.

iii) Solutions with $\beta \neq 0, \delta \neq 0$. In this more general situation, as may be verified, Eqs. 27–30 still admit two particular solutions for which

$$\hat{\Omega}(\tau) = (0, 0, -1), \quad \hat{\mathbf{a}}(\tau) = \pm \hat{\mathbf{b}}(\tau)/|\hat{\mathbf{b}}(\tau)|. \quad [38]$$

For these solutions, the mass m is again at rest on the vertical line passing through the center of the shell, either below the center (stable) or above it (unstable), corresponding, respectively, to the \pm in Eq. 38. In either situation, the rolling of the ball is synchronous with the rotation of the rotor in just such a way that the

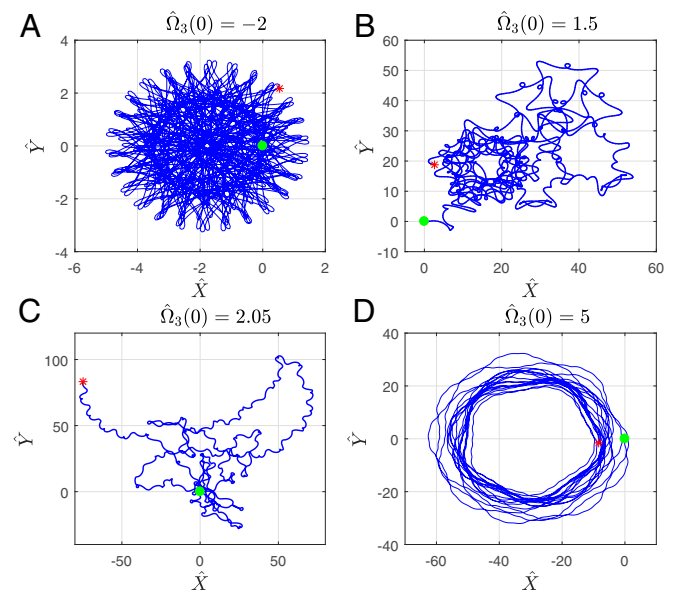


Fig. 5. (A–D) Trajectories $X(\tau)$ for $\mu = 2$, $\gamma = 4$, and $\bar{\beta} = 0.9$, $\bar{\delta} \approx 0.436$; $\hat{\mathbf{a}}(0)$ given by Eq. 41; $\hat{\Omega}(0) = (0, 0, \hat{\Omega}_3(0))$, with $\hat{\Omega}_3(0)$ as indicated; and Lyapunov exponents (A) $\lambda \approx 0.004$, (B) $\lambda \approx 0.084$, (C) $\lambda \approx 0.093$, and (D) $\lambda \approx 0.006$.

mass m remains stationary, exerting zero moment about C . The corresponding trajectories (Eq. 32) are straight lines.

Further Numerical Results

The following results were obtained by numerical solution of Eqs. 27 and 28, again using MATLAB. Writing Eq. 30 in the form

$$\hat{\mathbf{b}} = \rho(\tilde{\beta} \cos \tau, \tilde{\beta} \sin \tau, \tilde{\delta}), \quad [39]$$

where

$$\rho = |\hat{\mathbf{b}}| = \sqrt{\tilde{\beta}^2 + \tilde{\delta}^2}, \quad \tilde{\beta} = \beta/\rho, \quad \tilde{\delta} = \delta/\rho, \quad [40]$$

we now prescribe the motion of the mass m inside the shell in terms of ρ and $\tilde{\beta}$; ρ is the constant (dimensionless) distance $O'P$ of m from the center of the sphere and is fixed at $\rho = \frac{1}{2}$ in the computations that follow.

The initial value of $\hat{\mathbf{a}}$ is given in terms of the Euler angles $\{\theta_0, \phi_0, \psi_0\}$ at time $\tau = 0$ from Eq. 6; i.e.,

$$\hat{\mathbf{a}}(0) = (\sin \theta_0 \cos \psi_0, -\sin \theta_0 \sin \psi_0, -\cos \theta_0) \quad [41]$$

(and ϕ_0 can be chosen to be zero). It is supposed that the mass m moves according to Eq. 39 for $\tau \geq 0$. In Figs. 3–7, the trajectories $(\hat{X}(\tau), \hat{Y}(\tau))$ start at $(0, 0)$ (shown by a green circle) at time $\tau = 0$; they are computed for $0 < \tau < 300\pi$, i.e., for 150 periods of the motion of the mass m relative to the shell, the final point at $\tau = 300\pi$ being shown by a red asterisk.

The Lyapunov exponent λ was also computed for each trajectory, to detect sensitive dependence on initial conditions and possible chaos. For this purpose, we used the MATLAB code of Govorukhin (4), which computes the Lyapunov spectrum using the algorithm of Wolf et al. (5). In all examples studied here, we found that $\hat{\Omega}(\tau)$ was confined to a finite region of \mathbb{R}^3 containing the origin; since $\hat{\mathbf{a}}(\tau)$ is restricted to the unit sphere $|\hat{\mathbf{a}}| = 1$, the system therefore evolves in a finite region of \mathbb{R}^6 . In this situation, the occurrence of a positive Lyapunov exponent indicates chaotic behavior.

i) Trajectory of the Ball from a State of Rest with Mass m in Lowest Position. Consider first the situation where the shell is initially at rest and the mass m is at its lowest position:

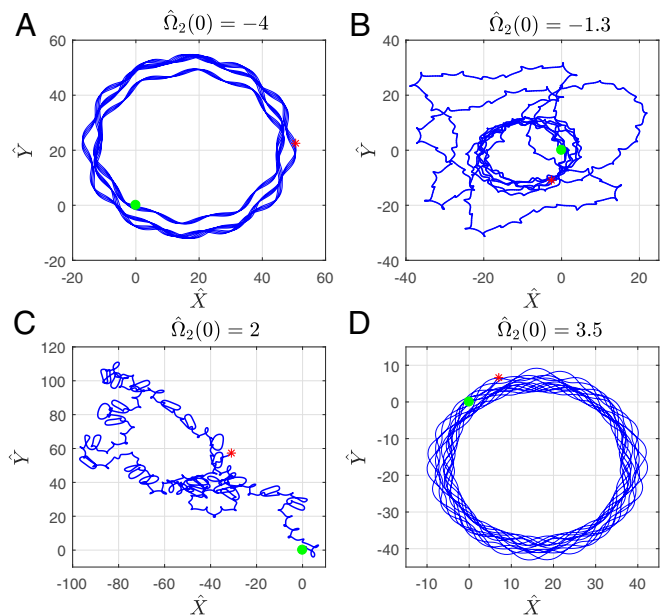


Fig. 6. (A–D) Same as Fig. 5, but with $\hat{\Omega}(0) = (0, \hat{\Omega}_2(0), -1)$, $\hat{\Omega}_2(0)$ as indicated, and (A) $\lambda \approx 0.005$, (B) $\lambda \approx 0.033$, (C) $\lambda \approx 0.103$, and (D) $\lambda \approx 0.005$.

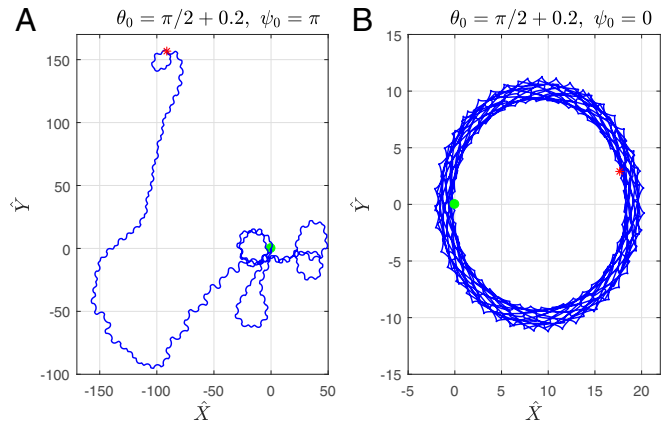


Fig. 7. Computed trajectories for parameter values $\mu = 4.6$, $\gamma = 3.2$, $\beta = 0.5$, $\delta = 0$. (A) trajectory starting with m near highest position, showing random behavior at least up to $\tau = 300\pi$. (B) Trajectory starting with m near lowest position, following a nearly circular path with oscillations of frequency σ . Note the difference of scale between A and B.

$$\hat{\Omega}(0) = 0, \quad \psi_0 = 0, \quad \text{and} \quad \theta_0 = \arccos(-\tilde{\delta}). \quad [42]$$

The computed trajectories $\{\hat{X}(\tau), \hat{Y}(\tau)\}$ are shown in Fig. 3. The Lyapunov exponents λ in the Fig. 3 legend are positive, but close to zero for Fig. 3 A and B and much larger for Fig. 3 C and D, consistent with the apparent chaotic character of the latter trajectories.

ii) Trajectory of the Ball from a State of Rest m in Highest Position. For this case, the initial conditions are

$$\hat{\Omega}(0) = 0, \quad \psi_0 = \pi, \quad \text{and} \quad \theta_0 = \arccos(-\tilde{\delta}), \quad [43]$$

and corresponding trajectories are shown in Fig. 4. Again, the relatively large positive values of λ in Fig. 4 C and D are consistent with the apparent chaos of the trajectories.[§]

iii) Effect of Nonzero $\hat{\Omega}(0)$ [and $V(0)$ Given by Eq. 13]. Fig. 5 shows the results with initial angular velocity $\hat{\Omega}(0) = (0, 0, \hat{\Omega}_3(0))$ for four different values of $\hat{\Omega}_3(0)$. In this case, λ is relatively large in Fig. 5 B and C, consistent again with the apparently chaotic trajectories. In the limiting situation $\hat{\Omega}_3(0) = -1$, the trajectory is a straight line along the y axis corresponding to the exact solution 38. Note here that not all values for $\hat{\Omega}_3(0)$ lead to solutions defined for all $\tau > 0$, because the contact condition 35 may fail for some $\tau = \tau_* > 0$. The computations show that Eq. 35 does actually hold at least up to $\tau = 300\pi$ provided $-5.96 \leq \hat{\Omega}_3(0) \leq 5.00$ (and fails just outside these limits).

If $\hat{\Omega}_3(0)$ is close to -1 , the trajectory is close to a circle. As $|\hat{\Omega}_3(0) + 1|$ increases from zero, the behavior becomes more interesting, as evident in Fig. 5, but when $\hat{\Omega}_3(0)$ approaches either end of the interval $[-5.96, 5.00]$, the motion becomes more regular; e.g., near the left end, the trajectory is almost circular. This is because the effect of the mass m is small when the initial angular velocity magnitude $|\hat{\Omega}(0)|$ is relatively large.

[§]Figs. 3 A and B and 4 A and B suggest the possible existence of invariant tori for small β (i.e., approximately near the integrable case $\beta = 0$); there is perhaps lurking here a nonholonomic counterpart of the Kolmogorov–Arnold–Moser (KAM) theorem for near-integrable Hamiltonian systems, a proposition that certainly deserves detailed investigation. We are grateful to a referee for this interesting suggestion.

